

First-principles study of the defect-activity and optical properties of FAPbCl₃

Sean Nations^a, Lavrenty Gutsev^{a,b}, Bala Ramachandran^a, Sergey Aldoshin^b, Yuhua Duan^c,
Shengnian Wang^{a*}

^a *Institute for Micromanufacturing, Louisiana Tech University, Ruston, LA 71272, United States*

^b *Institute of Problems of Chemical Physics of Russian Academy of Sciences, 1, Acad. Semenov
Av., Chernogolovka, Moscow region, 142432 Russian Federation*

^c *National Energy Technology Laboratory, United States Department of Energy, Pittsburgh,
Pennsylvania 15236, USA*

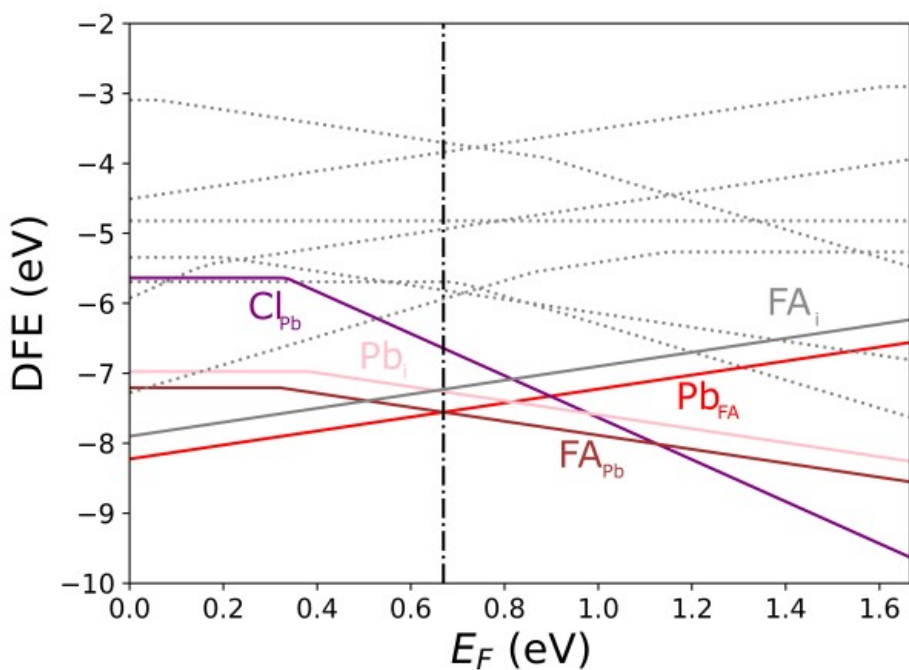
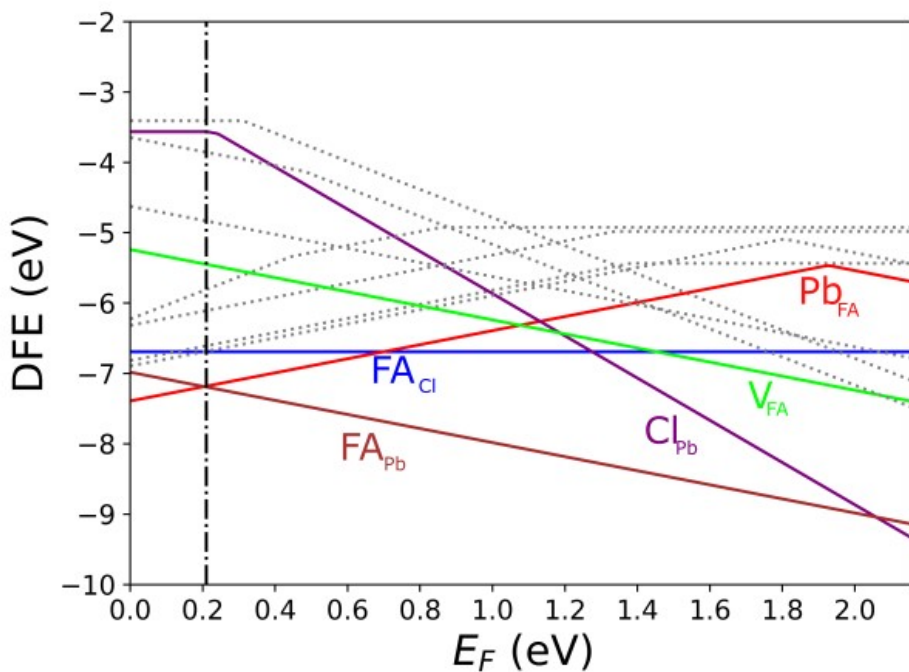


Figure S1. The calculated defect formation energy (DFE) as a function of the Fermi level for FAPbCl_3 . The vertical dashed line indicates the value of the Fermi level caused by the defect pair that controls the pinning. a) PBE+D3 with intermediate potentials at 0 K. b) SCAN+D3 with intermediate potentials at 0 K.

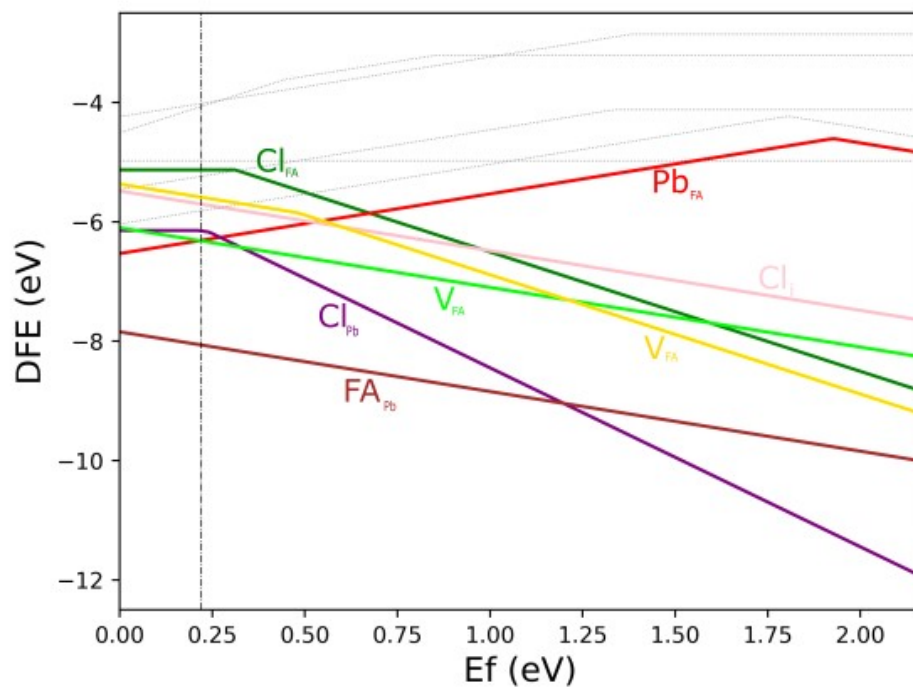


Figure S2: The PBE+D3 defect formation energy (DFE) for the Cl-rich case at 0 K as a function of the Fermi level for FAPbCl₃. The vertical dashed line indicates the value of the Fermi level caused by the defect pair that controls the pinning.

Optics:

The imaginary portion of the dielectric constant is obtained as a 3×3 Cartesian tensor as follows:

$$\varepsilon_2^{\alpha\beta}(\omega) = \frac{4\pi^2 e^2}{\Omega} \lim_{q \rightarrow 0} \frac{1}{q^2} \sum_{c,v,k} 2\omega_k \delta(\varepsilon_{ck} - \varepsilon_{vk} - \omega) \times \langle u_{ck + \varepsilon_{\alpha} q} | u_{vk} \rangle \langle u_{vk} | u_{ck + \varepsilon_{\beta} q} \rangle \quad (\text{S1})$$

where the summation is over indices c (CB states), v (VB states), and k (k-points), e is elementary charge, Ω is volume of the Brillouin zone, ω_k is weight of the k-point vector, ε_{ck} and ε_{vk} are energy levels, and u_{ck} is the periodic portion of the orbital at k-point k . Vector e_{α} is made of unit vectors for the Cartesian directions and α/β refer to axis x , y , and z . From the imaginary portion of the dielectric constant, the real part can be obtained by a Kramers-Kronig transformation:

$$\varepsilon_1^{\alpha\beta}(\omega) = 1 + \frac{2}{\pi} P \int_0^{\infty} \frac{\varepsilon_2^{\alpha\beta}(\omega') \omega'}{\omega'^2 - \omega^2} d\omega' \quad (\text{S2})$$

where P denotes the Cauchy principal value. As the dielectric tensor is diagonally dominate and with nearly identical diagonal elements, ε_1 and ε_2 are taken here to be the average of their three diagonal elements calculated via equations S1 and S2.

The real part of the optical conductivity ($\sigma(\omega)$) is defined as

$$\sigma_1(\omega) = \text{Re}[\sigma(\omega)] = \frac{\omega}{4\pi} \varepsilon_2(\omega) \quad (\text{S3})$$

where $\sigma(\omega)$ and ω are in the cgs unit of sec^{-1} . The cgs conductivity is 9×10^{11} times larger than the

SI conductivity unit (Siemens/cm) which in the form of $\sigma_1(\omega) = \frac{\varepsilon_2(\omega) \cdot \omega}{60}$ where ω is in the unit of cm^{-1} . The corresponding imaginary part of $\sigma(\omega)$ in SI unit is ²

$$\sigma_2(\omega) = - \frac{\omega(\varepsilon_1(\omega) - 1)}{60} \quad (\text{S4})$$

The complex dielectric constant can be expressed as:

$$\varepsilon(\omega) = \varepsilon_1(\omega) + i\varepsilon_2(\omega) = \frac{4\pi i}{\omega}\sigma(\omega) = (\tilde{n} + ik)^2 \quad (5)$$

where \tilde{n} and k are the index of refraction and the extinction coefficient respectively, and can be evaluated by the calculated dielectric constants from equations (S1) and (S2).

$$\tilde{n} = \frac{1}{\sqrt{2}}(\varepsilon_1 + (\varepsilon_1^2 + \varepsilon_2^2)^{\frac{1}{2}})^{\frac{1}{2}} \quad (6)$$

$$\tilde{k} = \frac{1}{\sqrt{2}}(-\varepsilon_1 + (\varepsilon_1^2 + \varepsilon_2^2)^{\frac{1}{2}})^{\frac{1}{2}} \quad (7)$$

In the case of normal incidence, the reflectivity R and the absorption coefficient α (sec^{-1} in cgs unit) in terms of \tilde{n} and k are defined as ²

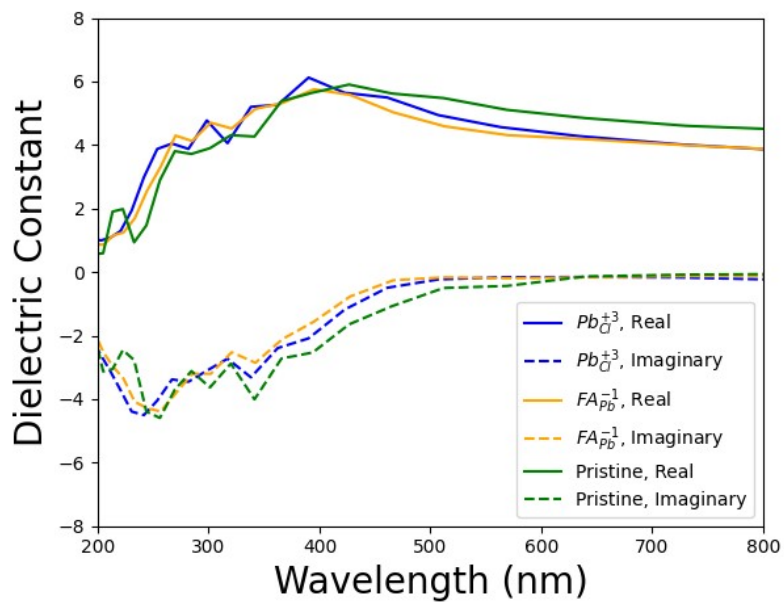
$$R = \frac{(\tilde{n} - 1)^2 + k^2}{(\tilde{n} + 1)^2 + k^2} \quad (8)$$

$$\alpha = \frac{2\omega k}{c} \quad (9)$$

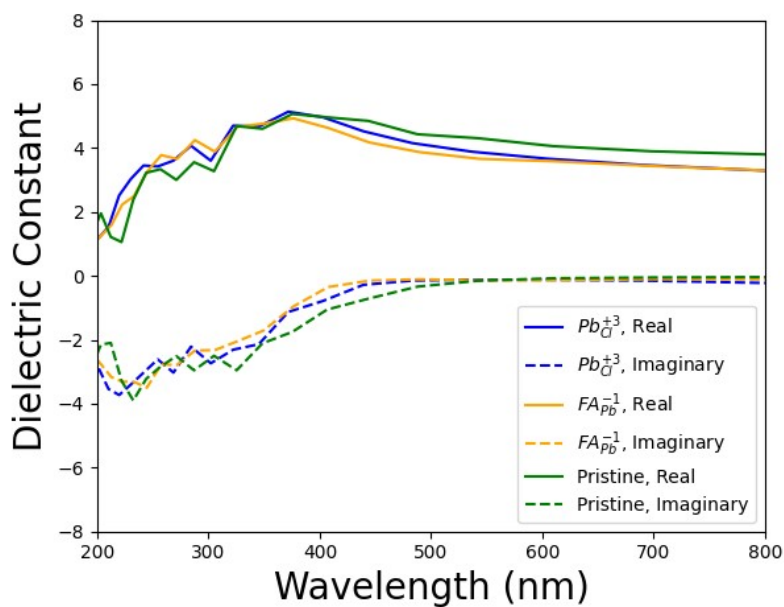
In SI unit, ω and α are in cm^{-1} , $\alpha = 4\pi\omega k$. In all cases, both the low frequency region $\omega\tau \ll 1$ (τ is the relaxation time) and the high frequency region $\omega\tau \gg 1$ are extensively studied to analyze the exact ground state of the material as these two regions carry the signatures of two distinct mechanisms associated with optical conductivity within a solid. While the low frequency region is dominated by free carriers which are in abundance in a metal, the high frequency region is dominated by inter-band electronic transitions typical of a dielectric material. As in the limit $\omega\tau \ll 1$, both \tilde{n} and k become sufficiently large, for example, in a metallic conductor,

$$R = 1 - \frac{2}{\tilde{n}} \rightarrow 1 \quad (10)$$

which means that the conductor is characterized by its behavior as a perfect reflector with an exceedingly large absorption coefficient in the low frequency region.

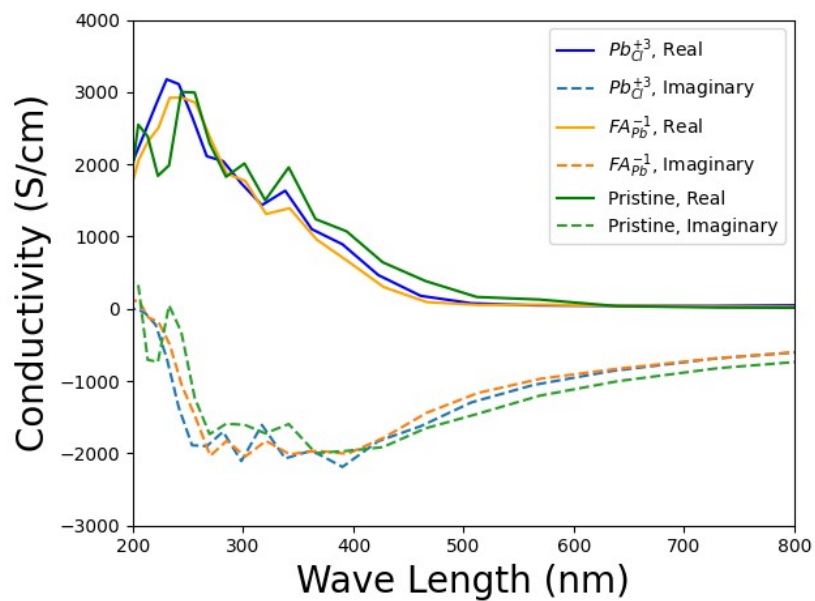


(a)

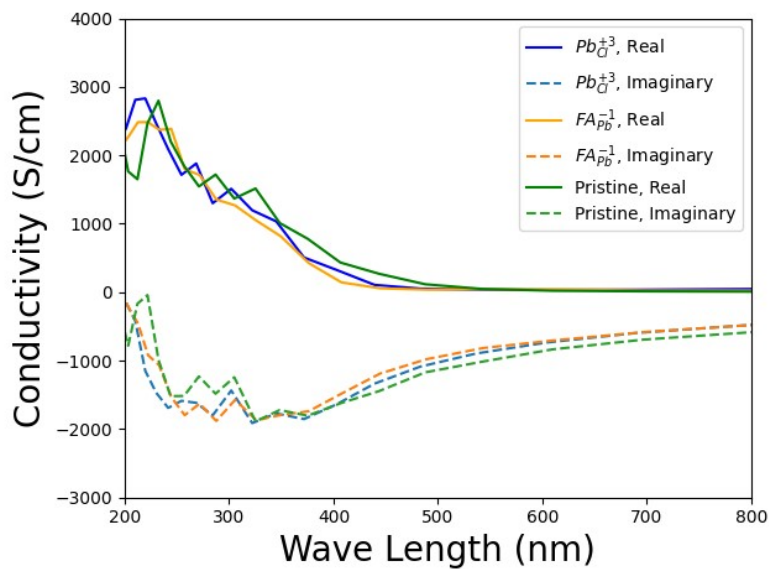


(b)

Figure S3. The complex dielectric constant for (a) PBE+D3 and (b) SCAN+D3 with the real portion plotted regularly and the imaginary portion plotted on the negative y-axis.

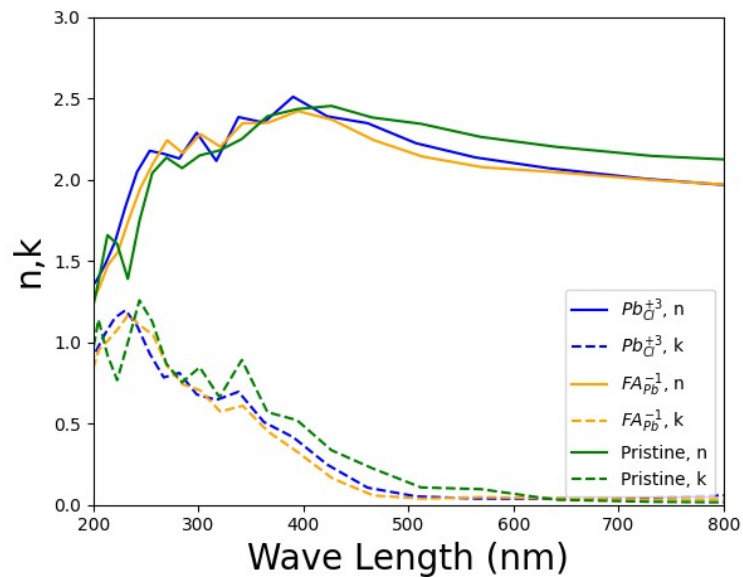


(a)

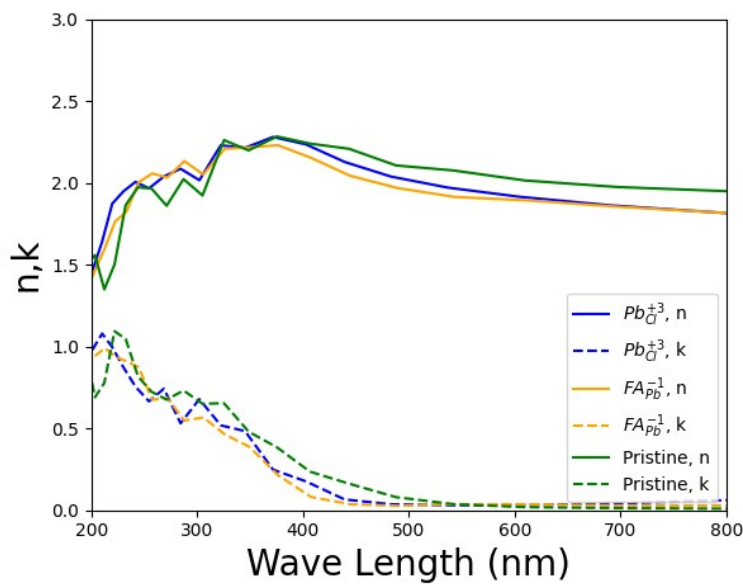


(b)

Figure S4. The complex conductivity for (a) PBE+D3 and (b) SCAN+D3.

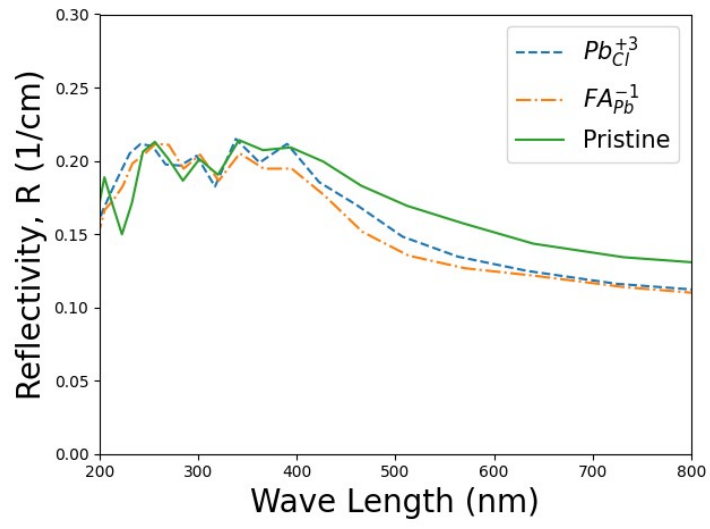


(a)

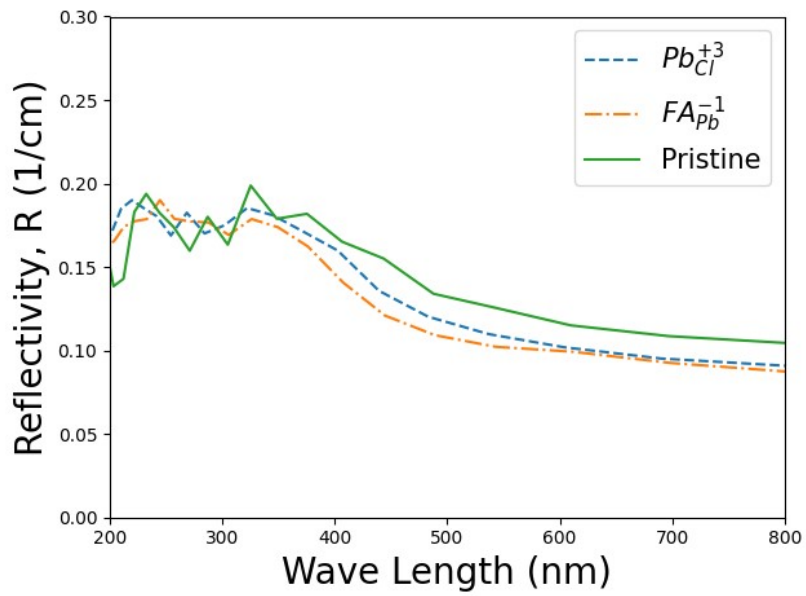


(b)

Figure S5. The refractive index (n) and extinction coefficient (k) for (a) PBE+D3 and (b) SCAN+D3.



(a)



(b)

Figure S6. The reflectivity for (a) PBE+D3 and (b) SCAN+D3.

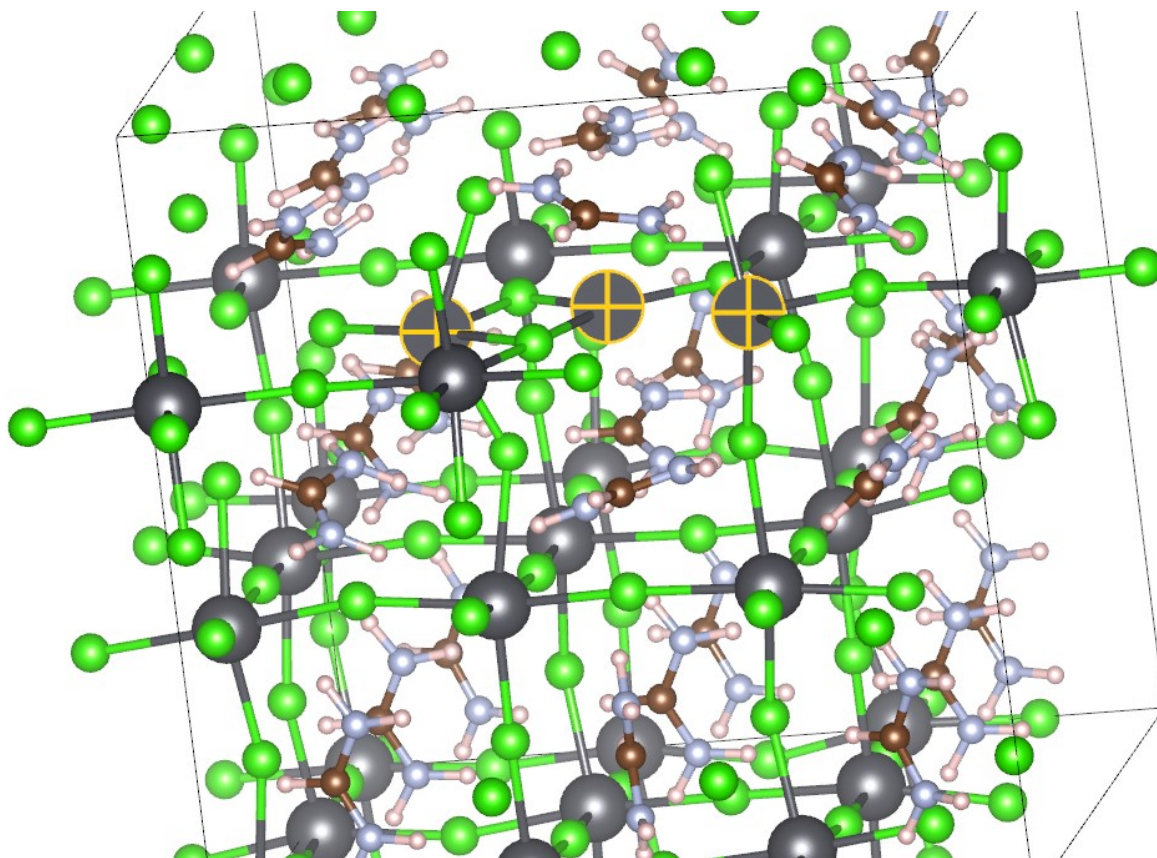


Figure S7. The local geometry of the Pb_{Cl} defect

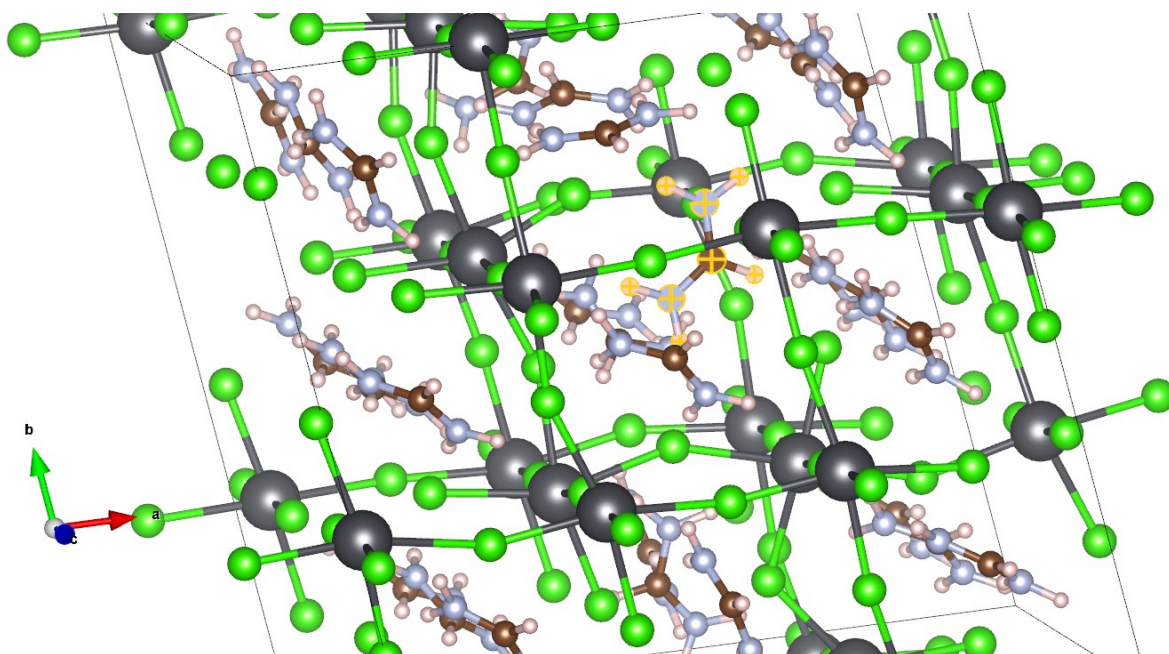


Figure S8. The local geometry of the FA_{Pb} defect

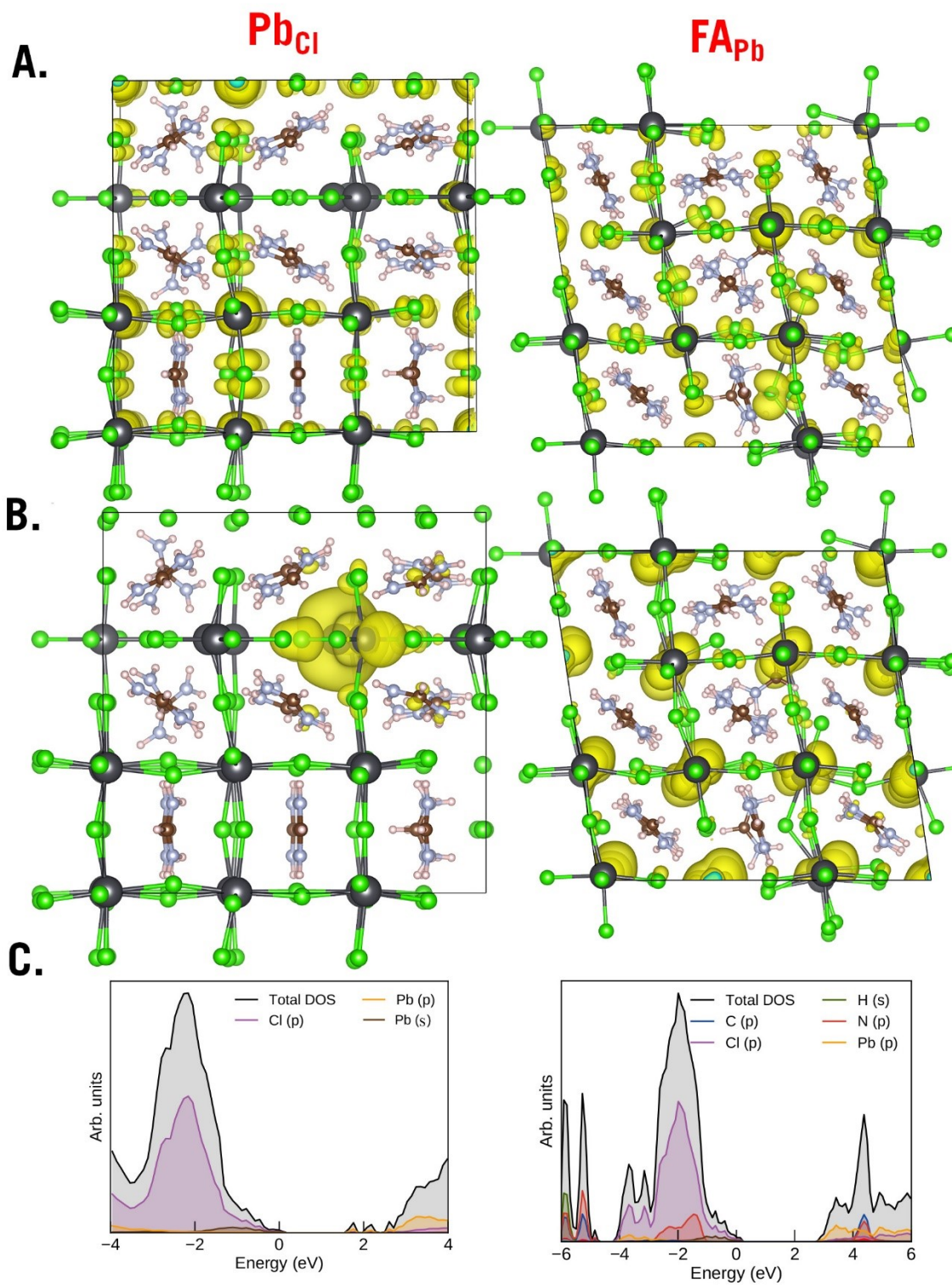


Figure S9. SCAN+D3 plots of A. HOMO, B. LUMO and C. DOS of the Pb_{Cl} and FA_{Pb} defects